

Molecular Packing and Lateral Interactions of Distearoylphosphatidylcholine with Dihexadecyldimethylammonium Bromide in Langmuir Monolayers and Vesicles

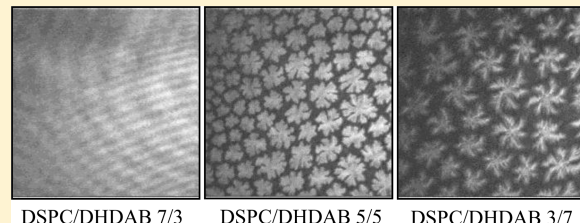
Chien-Hsiang Chang,[†] Chia-Hua Liang,[‡] Yu-Ying Hsieh,[†] and Tzung-Han Chou^{*§}

[§]Department of Chemical and Materials Engineering, National Yunlin University of Science and Technology, Yunlin 64002, Taiwan

[†]Department of Chemical Engineering, National Cheng Kung University, Tainan 701, Taiwan

[‡]Department of Cosmetic Science, Chia Nan University of Pharmacy and Science, Tainan 717, Taiwan

ABSTRACT: The behavior of distearoylphosphatidylcholine (DSPC) mixed with dihexadecyldimethylammonium bromide (DHDAB) in the monolayer was investigated by means of Langmuir trough, interfacial thermodynamic analysis, and Brewster angle microscopy. It was found that the cationic surfactant, DHDAB, was miscible with DSPC and a condensing effect, indicating stronger contraction of area per molecule and stronger ordering molecular packing, appeared in the mixed DSPC/DHDAB monolayers. Condensed structures of the mixed monolayers were visible as the molar fraction of DHDAB (X_{DHDAB}) ≤ 0.7 . The negative deviations of excess area and mixing Gibbs free energy were obtained, and their minimum values occurred at $X_{\text{DHDAB}} = 0.3$, suggesting that a DSPC/DHDAB monolayer with this composition exhibited the most pronounced intermolecular interactions with a compact molecular arrangement than the monolayers with separation between individual components. Furthermore, characteristics of mixed DSPC/DHDAB vesicles dispersed in water were studied by dynamic light scattering, transmission electron microscopy, and fluorescence polarization. The DSPC vesicles added with DHDAB showed zeta potentials of about +50 mV and narrower size distributions than those of pure DSPC vesicles. DSPC formed more rigid membranes than DHDAB, and the minimum disordering effect on membrane packing of vesicles was found at $X_{\text{DHDAB}} = 0.5$, which was the most stable vesicle composition against aggregation. By contrast, the condensing effect and the increase of intermolecular attraction in mixed DSPC/DHDAB monolayers may be related to the stability enhancement of mixed vesicles as compared with the stability of pure component vesicles.



INTRODUCTION

In the past two decades, cationic vesicles have caused great interest not only because of their capacity for drug delivery but also due to their utilization as a nonviral carrier for gene transfection.^{1–3} It is now widely recognized that vesicles composed of cationic surfactants with neutral phosphatidylcholines can successfully deliver negatively charged DNA into cells through electrostatic interactions.⁴ Nevertheless, cationic vesicles designed for DNA delivery usually exhibit low physical stability and undergo structural changes as interacting with cells.^{5,6} Most cationic surfactants for gene delivery system are toxic and have been reviewed by Lv et al.⁷ However, it has been found that the cytotoxicity of cationic surfactants in vesicles can be reduced by adding phosphatidylcholines.⁸ Cytotoxicity, gene transfection performance, and colloidal stability of these cationic vesicles are related closely to the vesicular constituents. Thus, finding out an optimal vesicular membrane composition of phosphatidylcholine/cationic surfactants for DNA delivery still deserves considerable attention.^{9,10}

The commonly utilized zwitterionic lipids for preparation of cationic liposomes are phosphatidylcholines or phosphatidylethanolamines and are able to increase efficiency of gene transfection with reduced cytotoxicity.^{1,11} Additionally, syn-

thetic cationic surfactants, dialkyldimethylammonium bromides, have been increasingly utilized due to their cationic phospholipid-like structure, low cost, and specific medically efficacy.^{12–14} Recently, the dispersion behavior of binary dipalmitoylphosphatidylcholine (DPPC)/dioctadecyldimethylammonium bromide (DODAB) vesicles formed by a simple vortex approach has been examined by size distribution, zeta potential, turbidity, and fluorescence polarization measurements.¹⁵ It has been revealed that the vesicle size decreased but zeta potential remained constant with increasing the DODAB mol %, and the maximum phase transition temperature (T_m) and colloidal stability were obtained at a composition of 50 mol % DODAB.¹⁵ The previous report by Linseisen et al.¹⁶ has also mentioned that DPPC vesicles containing 50 mol % DODAB expressed higher T_m than vesicles composed of each pure component. Montalvo et al.¹⁷ have found that only mixing lecithin/didodecyldimethylammonium bromide (DDAB) in water could form lamellar vesicles, and their structures and viscoelastic behavior depended on the composition. Therefore,

Received: November 22, 2011

Revised: January 20, 2012

Published: February 2, 2012

the manufacturing method and constituents of vesicles play significant roles in physicochemical properties of phospholipid/cationic lipid vesicles. Dihexadecyldimethylammonium bromide (DHDAB) can also form lamellar vesicles with positive charges¹⁸ and may be an appropriate cationic lipid for gene transfection and drug delivery purposes. Tucker et al.¹⁸ have deeply investigated the surface and solution properties of pure DHDAB by using small-angle neutron scattering, light scattering, neutron reflectivity, and surface tension and proven that DHDAB aggregates are in the form of lamellar vesicles with a high rigidity in the concentration range of 1.5–80 mM. However, the behavior of cationic DHDAB in mixtures with zwitterionic phospholipids is not fully understood. Distearoylphosphatidylcholine (DSPC) has longer double chains of C18 with a rather high T_m as compared with other phosphatidylcholines like DPPC and dimyristoylphosphatidylcholine (DMPC)¹⁹ and has been widely used as the major component for the preparation of artificial vesicles in drug and gene delivery due to its stability and nontoxicity.^{20,21} Here, DSPC is chosen to form cationic vesicles with DHDAB in order to get more useful information on the mixed cationic surfactant/phospholipid system (their chemical structures are shown in Figure 1).

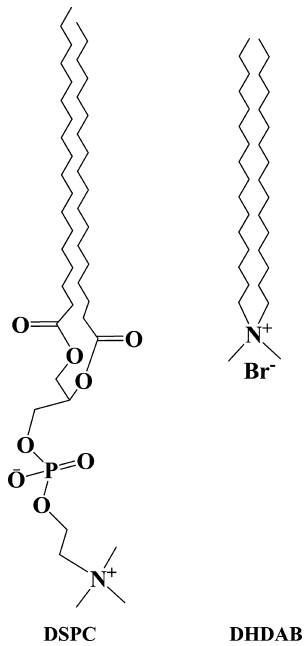


Figure 1. Chemical structures of zwitterionic distearoylphosphatidylcholine (DSPC) and cationic dihexadecyldimethylammonium bromide (DHDAB).

Generally, physicochemical characteristics of vesicular membranes are closely correlated to their delivery performance of genes or drugs.^{5,10,22} In this work, the mixed membrane properties of DSPC/DHDAB are investigated in order to provide useful information for applications of DSPC/DHDAB vesicles to drug or gene delivery in the future. The Langmuir monolayer approach is a very convenient and powerful tool to study the corresponding two dimensional characteristics of lipid bilayers since an insoluble monolayer can be acceptably considered as one-half of the lamellar biomembrane.²³ There have been progressively investigations on using monolayers of phosphatidylcholines at liquid surfaces as model systems to

realize the membrane behavior over the past several decades.²³ Some early work has been emphasized on the monolayer study involving DPPC with cationic lipids.^{24,25} It has been found that DPPC was miscible with DODAB, and mixed DPPC/DODAB monolayers expressed negative deviations from ideal mixing behavior.²⁴ However, a DPPC monolayer with the addition of a low mole fraction of 1,2-dioleoyl-3-trimethylammonium propane (DOTAP) displayed positive deviations from ideality.²⁵ The membrane behavior of phosphatidylcholines is strongly dependent on the addition of cationic surfactants. Nevertheless, a research regarding a DSPC monolayer mixed with DHDAB has not been addressed on the interfacial properties and molecular interactions at the air/water interface even if both of them have the potential as materials of a gene or drug carrier.

To understand the physicochemical behavior of a phospholipid/cationic lipid mixture, monolayer and vesicle membrane models are applied to characterize the molecular arrangement and interactions of DSPC and DHDAB in this study. First, this paper focuses on investigating the physicochemical behavior and morphology of mixed DSPC/DHDAB monolayers spread at the air/water interface at 24.5 °C. By means of surface pressure (π) and surface potential (ΔV) per molecule occupied area (A) isotherms with an interfacial thermodynamic analysis, the composition effect on the interfacial phase behavior of the mixed monolayers can be understood. In addition, the morphological characteristics of the mixed monolayers at different surface pressures can be directly observed by the Brewster angle microscopy. Second, vesicles composed of DSPC and DHDAB are prepared by the thin film hydration approach with subsequent sonication. A dynamic light scattering instrument is then used to evaluate the size distribution, zeta potential distribution, and storage stability of DSPC/DHDAB vesicles with various compositions. In addition, the fluorescence polarization technique is employed to study the packing and interactions between hydrocarbon chains in the vesicular bilayer. Finally, the effect of DHDAB on physicochemical characteristics of DSPC in the monolayer and vesicle is discussed. This study shows that DHDAB plays an important role in the structure organization, morphology, and thermodynamic stability of the lipid monolayer, and significantly contributes to the formation of small and stable lamellar lipid vesicles with positive charges.

EXPERIMENTAL SECTION

Materials. Distearoylphosphatidylcholine (DSPC) (>99%) was purchased from Avanti Polar Lipids (Alabaster, AL). Dihexadecyldimethylammonium bromide (DHDAB) (>98%) was obtained from Fluka (Buchs, Switzerland). The fluorescent probe 1,6-diphenyl-1,3,5-hexatriene (DPH) was received from Sigma-Aldrich. Ethyl alcohol (~99.5%) was supplied by Seoul Chemical Industry, Korea, and *n*-hexane of HPLC grade (99%) was obtained from Riedel-deHäen, Germany. A *n*-hexane/ethanol (9:1, v/v) mixture was used as the solvent for spreading monolayer-forming materials. Methanol and chloroform of HPLC analytical grade were obtained from Mallinckrodt Baker, Inc. (Phillipsburg, NJ). The phosphatidylcholine, cationic lipid, and solvents were utilized as received without further purification. The pure water with a resistivity of 18.2 MΩ cm obtained from a Milli-Q plus purification system (Millipore) was used in all experiments.

Monolayer Experiments. The sample solutions of DSPC/DHDAB mixtures were prepared according to the designed

molar ratios with a mixed *n*-hexane/ethanol (9:1, v/v) solvent, and the total concentration for each sample solution is fixed. The mixed DSPC/DHDAB monolayers were formed by spreading the sample solutions at the air/water interface on the Langmuir trough. A computerized Nima 601 trough system (Nima, England) equipped with a Brewster angle microscope (BAM: BAM2 plus, Nanofilm Technology Ltd., Germany) was used to obtain π -*A* and ΔV -*A* isotherms with the morphology information of the monolayers simultaneously at the interface. The trough having a working area of 7 cm × 70 cm was coated with polytetrafluoroethylene (Teflon) and was enclosed in an acrylic chamber on an isolated vibration-free table. The surface pressure was measured by the Wilhelmy plate method using a filter paper (1.0 × 2.4 cm²) provided by the trough manufacturer, while the surface potential was monitored with a Kelvin probe. A commercial BAM was utilized herein, and the detailed principle and design of the BAM have been described in the previous literature.²⁶

Before each run, the trough was washed with ethanol and rinsed with pure water. Then, the trough was filled with pure water as the subphase, and the temperature was controlled at 24.5 ± 1.0 °C by an external isothermal circulator. In order to confirm cleanliness of the initial air/water interface, the fluctuation of surface pressure is checked to be less than 0.2 mN/m during cyclic compression and expansion of the entire operated trough area. A desired quantity of the studied material in *n*-hexane/ethanol solvent was homogenously spread with a microsyringe onto the water surface, and a period of 20 min was waited for solvent evaporation. The monolayer was compressed symmetrically by two barriers at a constant rate of 2 Å²/(molecule-min). The π -*A* and ΔV -*A* isotherms were recorded, and BAM images were directly obtained during the continuous monolayer compression process. Experiments for each monolayer were carried out at least in triplication to confirm the reproducibility of the isotherm measurements within the deviation of 3 Å² per molecule.

Preparation of Vesicles. A mixture of DSPC and DHDAB in the designed molar ratio was weighed and dissolved into a mixed organic solvent of chloroform/methanol with a ratio of 1:1 by volume. The organic solvent was slowly withdrawn by reducing vapor pressure with a rotary evaporator at 50 °C for 1 h to gain a dried thin film on the wall of the round-bottomed flask. The mixed DSPC/DHDAB thin film was continued drying for 30 min under vacuum to completely remove the residual organic solvent. Then, the dried thin film was hydrated with pure water for 30 min at 60 °C to obtain multilamellar vesicles. After the hydration process, vesicles were sonicated at 60 °C with a power of 80 W to reduce the size by using a high performance ultrasonic machine (Sonicator 3000, Misonix Incorporation) equipped with a cup corn to avoid samples directly contacting with the titanium probe. The whole concentration for each mixed DSPC/DHDAB vesicle system was fixed at 10 mM.

Transmission Electron Microscopy. Electron micrographs were obtained by a transmission electron microscope (model H7500, Hitachi) with the negative-staining method. A 10 μL sample was applied onto a carbon grid and the grid stood for 10 min. Then, the excess sample was removed by means of a filter paper, and 10 μL of uranyl acetate solution was added. The grid was dried overnight in an auto drybox.

Size and Zeta Potential of Vesicles. Measurements of size and zeta potential distributions for mixed DSPC/DHDAB vesicles were performed at 25 °C using a Zetasizer NanoZS

instrument (Malvern Instruments Ltd., UK) equipped with a He–Ne laser and an optic detection with a scatter angle of 173°. The size (*d*) of vesicles was determined by the dynamic light scattering technique with photon correlation spectroscopy and was calculated by the Stokes–Einstein equation ($d = kT/3\pi\eta D$), where *k* is the Boltzmann constant, *T* is the absolute temperature, η is the solution viscosity, and *D* is the diffusion coefficient. Additionally, the zeta potential of vesicles was calculated from the electrophoretic mobility based on the Henry equation. All studied samples were not diluted for the size and zeta potential measurements.

Fluorescence Polarization Measurement. Vesicles were labeled by introducing a lipophilic fluorescent molecule, DPH. Aliquots of DPH dissolved in the mixed chloroform/methanol (1/1, v/v) solvent was added into the mixed DSPC/DHDAB stock solution, and then vesicles were prepared as described before. DPH was embedded in the lipid bilayers of vesicles, and the molar ratio of DPH:lipid was 1:1000. The steady-state fluorescence polarization measurements were performed at 25 °C using a Synergy 2 multimode microplate reader (BioTek Instruments, Inc.) controlled by BioTek's Gen5 reader control and data analysis software. The excitation wavelength was set at 360 nm, and the emission intensity at 430 nm was monitored. The fluorescence polarization values of the vesicle samples were calculated by the equation²⁷

$$P = \frac{I_{\text{par}} - GI_{\text{per}}}{I_{\text{par}} + GI_{\text{per}}} \quad (1)$$

where I_{par} and I_{per} indicate the fluorescence intensities polarized parallel and perpendicular, respectively, to the direction of polarization of the excitation beam, and $G = 0.87$ is the instrumental correction factor for optical variations between the parallel and perpendicular emission measurement paths. All experiments were done with multiple sets of samples, and average values of polarization were reported.

RESULTS AND DISCUSSION

Interaction of DHDAB and DSPC in the Langmuir Monolayer. Surface pressure–area per molecule (π -*A*) and surface potential–area per molecule (ΔV -*A*) isotherms of mixed DSPC/DHDAB monolayers with various DHDAB molar fractions (X_{DHDAB}) were simultaneously measured at the air/water interface at 24.5 °C and are illustrated in Figure 2. The π -*A* isotherm of a pure DSPC monolayer exhibited higher collapse pressure and steeper slope than that of a pure DHDAB monolayer, which indicated that DSPC could form a more condensed and less compressible Langmuir monolayer than DHDAB. Pure DHDAB with the positively charged headgroup might form a less ordered (i.e., liquid-expanded) monolayer on pure water. The π -*A* isotherms of pure DSPC and DHDAB monolayers did not exhibit the transition of liquid-expanded (LE) phase to liquid-condensed (LC) phase and were essentially consistent with those reported in the literature.^{28,29} Under the current experimental condition, 24.5 °C is below the main transition temperature of DSPC (54.8 °C)³⁰ and DHDAB (28 °C),³¹ pure DSPC and DHDAB monolayers were in the gel state corresponding to the lipid bilayer, perhaps resulting in smooth isotherms with no indication of a phase transition. With increasing the molar fraction of DHDAB in the mixed monolayers, the lift-off value of mean molecular area observed in the isotherms was shifted to the high value, and the collapse pressure was decreased. Generally, the π -*A* curve for a

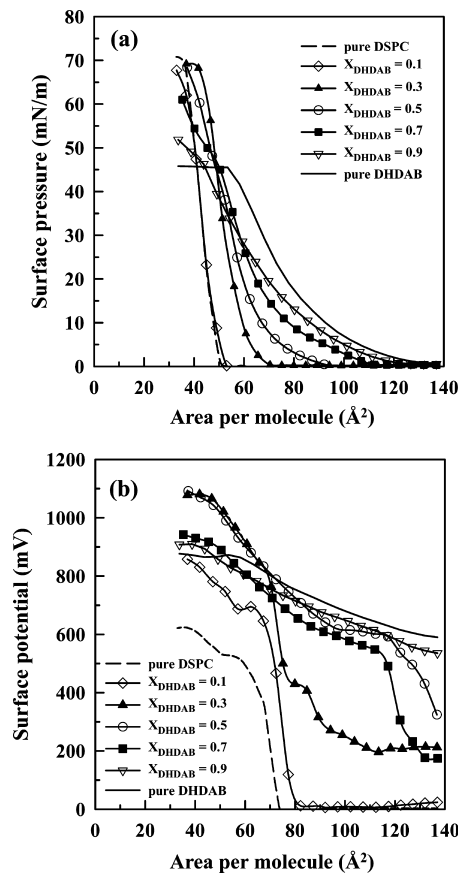


Figure 2. (a) Surface pressure–area per molecule and (b) surface potential–area per molecule isotherms of mixed DSPC/DHDAB monolayers with various compositions at the air/water interface at 24.5 °C.

condensed monolayer is steep and expresses a small lift-off area with a high collapse surface pressure. The results imply that adding high fractions of DHDAB into the DSPC monolayer decreases the molecular order of the film at the air/water interface. On the other hand, the DSPC rich monolayer exhibits the steep π -A curve, indicating that DSPC has a condensing effect for a DHDAB monolayer. DSPC has a longer dialkyl chain than DHDAB, and its zwitterionic headgroup may shield the electrostatic repulsion between the head groups of DHDAB, allowing molecules to arrange tighter in the mixed monolayer.

The molecular miscibility in a monolayer can be justified by utilizing the interface phase rule.³² If the two components are miscible at the air/water interface, collapse surface pressures of the mixed monolayers will vary with the composition. A monolayer composed of two immiscible materials will exhibit two distinctive collapse surface pressures corresponding to that of each pure component. Figure 2a shows that the collapse surface pressures of the mixed monolayers did change with the composition. It can be concluded that DSPC and DHDAB were miscible at the air/water interface. However, the addition of increasing amounts of the liquid-expanded DHDAB in the highly condensed DSPC monolayer did not result in the appearance of a clearly LE–LC phase transition, even though the experimental temperatures is closed to the phase transition temperature of DHDAB (28 °C).³¹ Similar findings were also observed for mixed DMPC/C16:0-ceramide monolayers.³³

The influence of composition on the average surface dipole moment of molecules in mixed DSPC/DHDAB monolayers can be observed with the ΔV –A isotherms (Figure 2b). At large occupied areas per molecule, the surface potential of a pure DHDAB monolayer is about 600 mV and higher than that of a pure DSPC monolayer (closed to 0 mV), which is attributed to the headgroup of the cationic surfactant. A nonzero surface potential for a monolayer at large molecular occupied areas has also been found in the literature, and the dipole moment contribution from a Gouy–Chapman double layer is considered as a major factor.³⁴ The increase in surface potential for a pure DHDAB monolayer under compression is less sharp than that for a pure DSPC monolayer. These imply that DSPC forms a condensed monolayer while DHDAB forms an expanded monolayer. In a DHDAB rich monolayer, ΔV –A curves shifted up and the slope became less steep. This suggested that the presence of rich DHDAB could provide a higher electrostatic repulsive force to disturb the orientation of DSPC in a mixed monolayer. These findings coincided with the results of π -A isotherms. However, ΔV –A isotherms of mixed monolayers with $X_{DHDAB} = 0.3, 0.5$, and 0.7 showed the state transition region from 80 to 130 Å² per molecule, which cannot be found in π -A isotherms. This suggested that deducing phase behavior only by π -A isotherms may be not enough due to the limit of the instrumental sensitivity. In addition, $\Delta V_{\text{collapse}}$, defined as the difference of surface potentials for a monolayer on the clean surface and at collapse, is related to the decrease of double-layer effect and increase of effective dipole moment perpendicular to the surface. The maximum of $\Delta V_{\text{collapse}}$ was observed at $X_{DHDAB} = 0.3$, resulting from the optimization of electrostatic interaction of head groups and van der Waals force of hydrophobic chains.

To further quantitatively realize the miscibility and interaction between two components in a monolayer, interfacial thermodynamic characteristics should be evaluated. First, the excess area (A_{ex}), which was applied to elucidate the molecular interaction for binary constituents in a monolayer, can be obtained by eq 2 at a given surface pressure.^{32,35,36}

$$A_{\text{ex}} = A_{12} - A_{\text{ideal}} = A_{12} - (X_1 A_1 + X_2 A_2) \quad (2)$$

where A_{12} and A_{ideal} are the actual occupied and ideal areas per molecule of the mixed monolayer, respectively, at a given surface pressure. A_1 and A_2 denote the areas per molecule of each pure monolayer at the same surface pressure, and X_1 and X_2 imply the respective mole fractions in the mixed monolayer. When $A_{\text{ex}} = 0$, ideal mixing occurs or the two components are completely immiscible in a monolayer. Otherwise, negative or positive values of A_{ex} indicate that two components are miscible and form nonideal mixed monolayers.

Figure 3a depicts the A_{ex} versus X_{DHDAB} for mixed DSPC/DHDAB monolayers at various surface pressures. All mixed DSPC/DHDAB monolayers exhibited negative area deviations from ideality, and the most significant deviation occurred at $X_{DHDAB} = 0.3$. This indicates that the appropriate addition of DHDAB into a DSPC monolayer could influence the electrostatic interactions of the head groups and make the molecular packing more condensed, especially at $X_{DHDAB} = 0.3$. This also proved the occurrence of condensing effect in mixed DSPC/DHDAB monolayers. A similar phenomenon has also been found in the area per lipid behaviors of mixed dimyristoylphosphatidylcholine (DMPC)/dimyristoyltrimethylammonium propane (DMTAP)³⁷ and mixed DMPC/

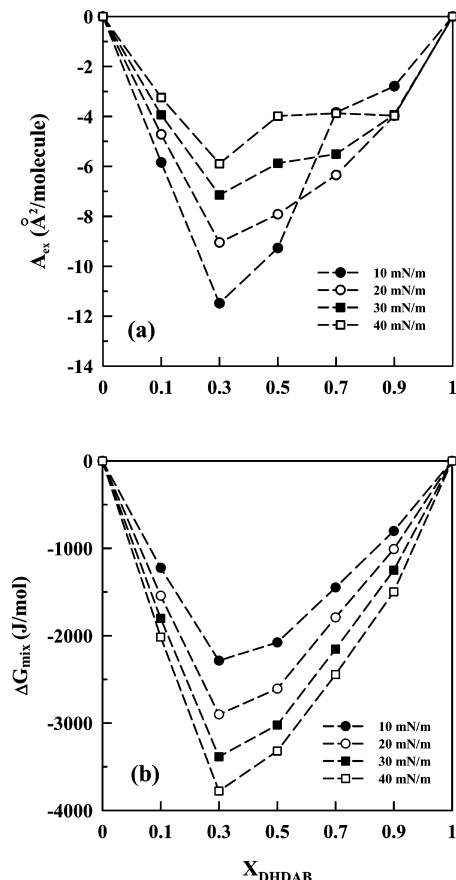


Figure 3. (a) Excess area, A_{ex} and (b) free energy change of mixing, ΔG_{mix} as a function of composition for mixed DSPC/DHDAB monolayers at the air/water interface at various surface pressures.

dioleoyltrimethylammonium propane (DOTAP)³⁸ systems by atomistic molecular dynamics simulation of lipid bilayers. The minima of area per lipid (maximum in ordering) were found for a DMPC bilayer with the DMTAP fraction of 0.5 and with the DOTAP fraction of 0.4, respectively, which may be due to the reorientation of the polar headgroup of DMPC in the presence of cationic lipids. Säily et al.³⁹ reported that the condensation effect in the mixed 1-palmitoyl-2-oleoyl-sn-glycero-3-phosphocholine (POPC)/sphingosine monolayers but found three critical mole fractions X_{Sph} of sphingosine, viz., 0.25, 0.6, and 0.83, at which the area/molecule reached a local minimum. The difference is possibly due to a larger volume of the unsaturated side chain of POPC as compared with completely saturated dialkyl chains of DMPC and DSPC. Besides, the magnitude of the negative deviations decreased with increased surface pressure, which can be anticipated since the monolayers were more compact at higher surface pressures and the effect of intermolecular interactions on molecular occupied area became less significant.

In addition, the thermodynamic stability of a mixed monolayer compared with an unmixed monolayer with separately individual components can be investigated from the calculation of the Gibbs free energy of mixing, ΔG_{mix} ^{32,35,36} which is given by

$$\Delta G_{mix} = N_A \int_0^\pi [A_{12} - (X_1 A_1 + X_2 A_2)] d\pi + RT(X_1 \ln X_1 + X_2 \ln X_2) \quad (3)$$

where N_A is the Avogadro number, R is the gas constant, and T is the absolute temperature. Treating data from the π - A isotherms by eq 3 gave the ΔG_{mix} of mixed DSPC/DHDAB monolayers as a function of composition at various surface pressures, which is shown in Figure 3b. The values of ΔG_{mix} for mixed monolayers with all compositions were negative, and no obvious phase separation or partially miscible phenomenon was suggested in the entire range of X_{DHDAB} in mixed DSPC/DHDAB monolayers at different surface pressures. This result indicates that the mixed monolayers were more stable than the corresponding unmixed monolayers consisted of separated individual components, especially at $X_{DHDAB} = 0.3$, suggesting such a configuration may minimize the repulsive electrostatic interactions between the cationic head groups of DHDAB. This nonideal mixing behavior of mixed DSPC/DHDAB systems is also found in the mixed micellar systems of nonionic and ionic surfactants. Mixed nonionic and ionic surfactants showed negative beta parameters associated with a net attraction and significant deviations from ideal behavior.^{40,41} Besides, the more negative values of ΔG_{mix} were observed at higher surface pressures, implying that the mixing of this binary system at higher surface pressures was more favorable than at lower surface pressures. The miscibility and the negative excess free energy change of mixing has been found for the mixed DPPC/DODAB system,²¹ but the minimum of negative excess free energy change of mixing occurred at $X_{DODAB} = 0.6$. Although the dialkyl chain length (2C16–2C18) for the mixed DPPC/DOAB system is identical to the mixed DSPC/DHDAB system, the mismatch in the relative location of cationic head groups in the monolayer obviously affects the monolayer behavior.

Brewster Angle Microscope Observation. Brewster angle microscopy was utilized herein to directly monitor the phase behavior of mixed DSPC/DHDAB Langmuir monolayers at various surface pressures at 24.5 °C, and the images are shown in Figure 4. One can find that the texture and morphology of the mixed monolayers varied with surface pressure and composition. No macroscopic domains can be found at the initial compression stage for all compositions under study (figures not shown). Figure 4 (the left column) displays the BAM images of the mixed monolayers with various compositions at low surface pressures ($\pi \leq 5 \text{ mN/m}$, $\sim 85 \text{ \AA}^2$ per molecule). A pure DSPC monolayer exhibited obvious condensed domain formation in the gas phase state of the π - A isotherm, but not for a pure DHDAB monolayer. The condensed (solid or liquid-condensed) domains with various shapes appeared under a low surface pressure were found as the mixed monolayers with $X_{DHDAB} \leq 0.7$. Flores et al. also found similar observation for a pure doctadecylamine (DODA) monolayer at pH = 3 at low temperatures.⁴² Although the LE-LC phase was not visualized in π - A isotherms, BAM images of mixed monolayers with $X_{DHDAB} = 0.5$ or 0.7 revealed the formation of cloverleaf-like domains at low surface pressures. Similar observations were found in the mixed DMPC/C14:0-ceramide monolayers.⁴³ For the mixed monolayers with $X_{DHDAB} > 0.7$ at low π , the bright domains present in a pure DSPC monolayer disappeared in the images. The decrease of bright domains confirmed the loose structure in the two-dimensional monolayers with high DHDAB mole fractions. Therefore, incorporation of high molar fraction of DHDAB into a DSPC monolayer indeed gave an electrostatic repulsion to disorder the molecular packing, which can be supported by the finding from the π - A and ΔV - A isotherms (Figure 2). Cárdenas et

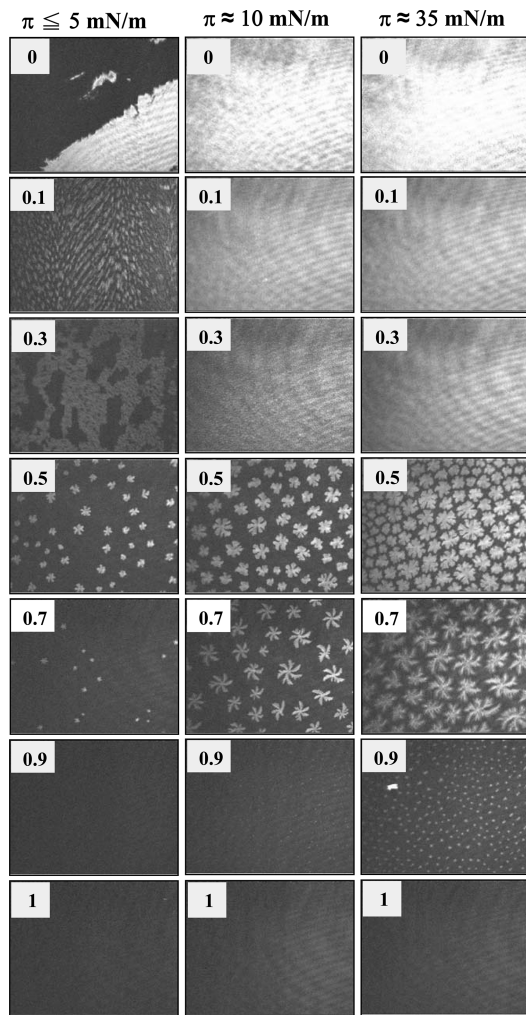


Figure 4. BAM images of mixed DSPC/DHDAB Langmuir monolayers with $X_{\text{DHDAB}} = 0, 0.1, 0.3, 0.5, 0.7, 0.9$, and 1 at surface pressures $\pi \leq 5 \text{ mN/m}$ (the left column), $\approx 10 \text{ mN/m}$ (the middle column), and $\approx 35 \text{ mN/m}$ (the right column) at 24.5°C . All images have the same scale of $387 \mu\text{m} \times 290 \mu\text{m}$. The interference patterns in the top 9 images are artifacts of the measurement and not a real characteristic of the monolayers studied.

al.⁴⁴ have found that the mixed DSPC–DODAB monolayers with 1:1 molar ratio on 25°C 2 mM NaBr aqueous solution at $\pi = 5 \text{ mN/m}$ formed a heterogeneous film with large condensed domains, whose shape is very different from that of the 1:1 molar ratio mixed DSPC/DHDAB monolayers at the same surface pressure. The image of a pure DSPC monolayer on 2 mM NaBr aqueous solution was less distinct than that on pure water observed in this report, possibly resulting from ions disturbance.⁴⁴ These results suggest that the dialkyl chain length of cationic surfactants and subphase solution strongly affect the monolayer morphology at the interface as the polar head groups of the mixed surfactant/lipid monolayers are identical. Besides, Lawrence et al. reported similar BAM image of fairly homogeneous surface at low surface pressure, except in the regions of phase transition, for a pure DODAB monolayer at 22°C .⁴⁵ They also found that the incorporation of DODAB into a dioleoylphosphoethanolamine (DOPE) monolayer increased the hydration and induced lateral phase separation, which is similar to the finding for mixed DSPC/DHDAB monolayers.⁴⁵

With further compressing the mixed monolayers, the interfacial molecules were pushed into a more compact state owing to the reduction of monolayer-occupied area at the air/water interface. Figure 4 (the middle column) displays the BAM images of the mixed DSPC/DHDAB monolayers with different compositions at a surface pressure of $\sim 10 \text{ mN/m}$ (at liquid-expanded state). In comparison with images observed at $\pi \leq 5 \text{ mN/m}$, one can find that the dark background disappeared and bright domains occupied over the images for the mixed monolayers with $X_{\text{DHDAB}} \leq 0.3$. For the mixed monolayers with $X_{\text{DHDAB}} = 0.5$ and 0.7, the bright branched domains grew in size and the domains showed a rotational symmetry but no reflection symmetry. Such rotational symmetry may be related with chirality, i.e., in the orientation that the molecule position is different from clockwise to counterclockwise. Only few condensed phase domains were observed in the monolayer with $X_{\text{DHDAB}} = 0.9$, but a pure DHDAB monolayer did not express obviously condensed domains. Upon progressively compressing to a surface pressure of $\sim 35 \text{ mN/m}$ (belong to solid state), the morphological changes of the mixed monolayers with various compositions are demonstrated in Figure 4 (the right column). The brightness and denseness of the homogeneous condensed domains increased slightly for monolayers with $X_{\text{DHDAB}} = 0, 0.1$, and 0.3 at the high surface pressure. The domain size grew and the branches and numbers of domains increased for mixed monolayers with $X_{\text{DHDAB}} = 0.5$ and 0.7 that expressed cloverleaf-like morphology. However, small bright dot domains became visible for the monolayer with $X_{\text{DHDAB}} = 0.9$ at the high surface pressure. The addition of DHDAB with DSPC monolayer ($X_{\text{DHDAB}} \leq 0.7$) showed bright condensed domains, perhaps attributed to the condensing effect evidenced by the A_{ex} calculations. The trends of these shapes and numbers of domains varying with surface pressure, which were related to the increase in the surface density, were similar to the finding for other monolayer systems.^{26,29}

Moreover, the 2-D aggregated domain shape of the monolayers changed from sheet-like to dots with increasing DHDAB mole fraction in the mixed monolayers. Such topological changes resulted from a decrease in the dispersion interaction between alkyl chains due to the addition of comparatively shorter alkyl chains of DHDAB and an increase in the electrostatic repulsive force between polar head groups of the components, as X_{DHDAB} was increased in the mixed monolayer system. The group of McConnell has widely studied the lipid monolayer morphology by using fluorescence microscopy and developed theories in attempts to explain the various shape changes of lipids domains.^{46,47} The most acceptable theory to date is based on the competition between electrostatic repulsion and line tension,⁴⁷ which also may help explain the finding here. Furthermore, Karttunen et al.⁴³ observed lipid domain morphologies in DMPC-ceramide monolayers by fluorescence microscopy and found that the shape of solid domains changed with the N-acyl chain length of ceramide.⁴³ It is interesting that the morphological images of mixed DMPC/ceramide with N-acryl chain length of 14/NBD-PC (66:33:1) monolayers and the increased LC phase coverage under compression of mixtures were very similar to that for a mixed DSPC/DHDAB monolayer with $X_{\text{DHDAB}} = 0.5$ or 0.7. They found that DMPC with shorter ceramides formed flower-like domains, whereas DMPC with longer ceramides formed round domains. These results suggested that the increased electrostatic repulsion of headgroups and the decreased van der

Waals interaction in a mixed monolayer resulted in the appearance of branched domains. Flores et al. also investigated the morphologies of dioctadecylamine, ethyl palmitate, and ethyl stearate monolayers at specific pH by Brewster angle microscopy. They also observed similar dendritic domains in the DODA monolayer, resulting from the line tension anisotropy.^{42,48}

Physicochemical Characteristics and Physical Stability of Vesicles.

Morphology of vesicles composed of 90 mol % DSPC and 10 mol % DHDAB was observed by a transmission electron microscope (Figure 5). One can find the presence of

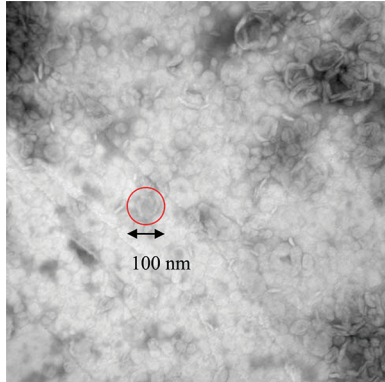


Figure 5. Image of mixed DSPC/DHDAB (9/1, molar ratio) vesicles obtained by a transmission electron microscope. The total lipid concentration in the vesicle dispersion is 10 mM.

spherical vesicles with a diameter of <200 nm and the bilayer structures of disrupted vesicles. Size distribution and zeta potential measurements are often used to determine the vesicle characteristics in aqueous dispersions. In Figure 6, the initial size and zeta potential distributions of mixed DSPC/DHDAB vesicles with various X_{DHDAB} are demonstrated. Pure DSPC vesicle dispersions showed a larger average vesicle size with a wider size distribution. Adding 10–90 mol % DHDAB ($X_{\text{DHDAB}} = 0.1$ –0.9) into DSPC vesicles seemed to reduce the hydrodynamic diameter distribution (Figure 6a). The size distribution of pure DHDAB vesicles here was consistent with the work reported by Tucker et al.¹⁸ They showed that the DHDAB vesicles are relatively polydisperse with a particle size in the range 200–400 nm with the concentration range 1.5–80 mM. Furthermore, a net positive charge (5–60 mV) was observed for all mixed DSPC/DHDAB vesicle formulations (Figure 6b). As incorporating DHDAB into DSPC vesicles ($X_{\text{DHDAB}} \geq 0.1$), the zeta potential of cationic vesicles was significantly increased and approached the value of about 40–60 mV, which was basically independent of the DHDAB mole fraction. This may be because that DHDAB having a high ionic dissociation degree made the surface charge density of vesicles quickly saturated. Yokoyama et al.⁴⁹ have found that the addition of dipalmitoyldimethylammonium bromide (DPAB) into DPPC vesicles could form a large unilamellar vesicle (500 nm–2 μm) with a zeta potential of ~40 mV by using a simple vortex method. In this study, smaller cationic vesicles formed by strong sonication may have a higher surface charge density than larger vesicles, resulting in a higher surface potential. By comparison, the asymmetry in chain length might give the molecules possibility to pack and align so as to give a higher charge.

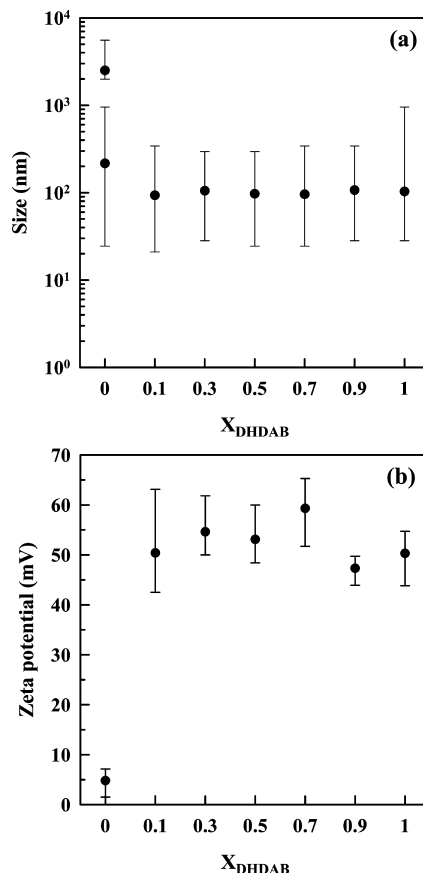


Figure 6. (a) Hydrodynamic diameter and (b) zeta potential distributions as a function of composition for mixed DSPC/DHDAB vesicles in pure water. The total lipid concentration is 10 mM. Each measurement is carried out with at least three independent experiments, and the standard deviation is below 5%. The black dot in the distribution line indicated the average value for each composition.

Fluorescence polarization is a commonly used method to evaluate molecular packing order of lipid membranes.⁵⁰ A lipophilic fluorescent probe, DPH, incorporated into the deeper lipid bilayer can provide information about the molecular arrangement of the hydrophobic regions because the probe has a greater rotation freedom in a loosely packing state of lipids.⁵¹ Figure 7a illustrates the fluorescence polarization degree of mixed DSPC/DHDAB vesicles as a function of composition at 24.5 °C, which is below the phase transition temperature of DSPC (54.8 °C)³⁰ and DHDAB (28 °C).³¹ The polarization value of pure DSPC vesicles, 300 mP, was higher than that of pure DHDAB vesicles (150 mP). This implied that molecular packing of a DHDAB membrane was more fluidized than that of a DSPC membrane, apparently because DHDAB has a shorter dialkyl chain than DSPC and a polar headgroup with positive surface charges providing strong electrostatic repulsive interactions. In addition, a maximum of polarization value appeared at $X_{\text{DHDAB}} = 0.5$, which indicated that the vesicular bilayer with this composition exhibited highest order in the molecular arrangement and the membrane was the most rigid. Therefore, one can conclude that the molecular fluidity of vesicle membranes decreased with X_{DHDAB} from 0 to 50 mol % and then increased with X_{DHDAB} from 50 to 100 mol %. The effect of small DHDAB addition (<50 mol %) on decreasing the packing disorder of the hydrophobic chains of DSPC/

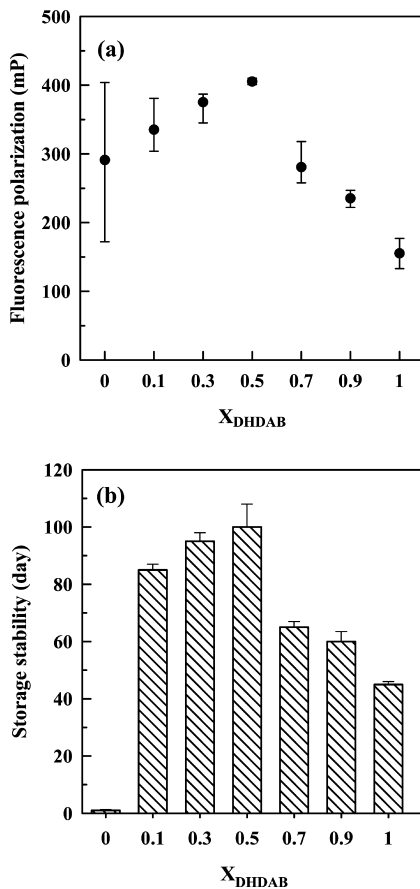


Figure 7. (a) Fluorescence polarization and (b) storage stability at room temperature as a function of composition for mixed DSPC/DHDAB vesicles in pure water. The total lipid concentration is 10 mM. The time span for each stability measurement is 5 days. The storage stability criterion: As the average particle size >600 nm or polydispersity (PI) > 0.7 for the dispersion, vesicles are considered to be unstable.

DHDAB vesicles is similar to the condensing effect of DHDAB mixed with a DSPC monolayer at the air/water interface. This can be realized from the isotherms, the excess areas, and BAM images of mixed DSPC/DHDAB monolayers, although the most pronounced effect on molecular packing appeared at $X_{\text{DHDAB}} = 0.3$, which is close to a ratio of 1:2. Besides, Sobral et al.¹⁵ have found that a maximum value of the phase transition temperature of large DPPC/DODAB vesicles occurred at $X_{\text{DPPC}} = 0.6$. However, the highest phase transition temperature for the binary DPPC/DPAB system appeared with the molar fractions of DPAB from 0.25 to 0.3.⁴⁹ The symmetry in the dialkyl chains of lipids seems to affect the behavior and characteristics of these mixed systems, resulting in the difference of the optimum compositions. Therefore, the membrane constituent plays an important role in the vesicle characteristics, and these phenomena indicated that the optimization between the electrostatic interaction of the head groups and the van der Waals force of dialkyl chains determined the molecular packing order of the membranes.

Figure 7b shows the physical stability of mixed DSPC/DHDAB vesicles as a function of X_{DHDAB} , which is determined by vesicle size (<400 nm), polydispersity (<0.4), or optical observation (no aggregates or no phase separation). One can find that physical stability of the vesicles increased as X_{DHDAB} changed from 0 to 0.5 but obviously decreased as $X_{\text{DHDAB}} > 0.5$.

The storage physical stability is generally considered to be affected by both intervesicle interactions and intravesicle interactions. Pure DSPC vesicles had a large average size, a wide size distribution, and near zero zeta potential at the beginning (Figure 6), resulting in the poorest vesicle stability. Pure DHDAB vesicles had small average size with initial zeta potential of ~50 mV that provided an electrostatic repulsion between vesicles and the highest molecule mobility in the vesicle membrane among the others (Figure 7a). The enhancement of physical stability was observed for mixed DSPC/DHDAB vesicles as compared with the stability of vesicles of the pure components, possibly arising from the increase of the interactions (or rigidity) and the occurrence of condensing effect in the mixed DSPC/DHDAB systems. Furthermore, the most stable vesicles with a composition of $X_{\text{DHDAB}} = 0.5$ showed a small particle size, a narrow size distribution, a zeta potential of ~52 mV, and the highest rigidity of intrabilayers (Figures 6 and 7). This suggests that the highest storage stability of vesicles is related to the optimization between intervesicle and intravesicle interactions.

CONCLUSIONS

π -A and ΔV -A isotherms of mixed DSPC/DHDAB monolayers were obtained with BAM observation of the monolayer morphology at the air/water interface at 24.5 °C, and the interfacial thermodynamic analysis for mixed DSPC/DHDAB monolayers was further carried out. DSPC was miscible with DHDAB in the Langmuir monolayers and showed a condensing effect in the mixed DSPC/DHDAB monolayers. The monolayer with $X_{\text{DHDAB}} = 0.3$ expressed the minima of A_{ex} and ΔG_{mix} , implying that a monolayer with this composition had the tightest packing and was more stable thermodynamically than the monolayers with separation between individual components. The BAM observation suggested that appropriate addition of DHDAB with a DSPC monolayer resulted in the occurrence of condensed domains and the phase domain shape depended on the composition.

In the case of mixed DSPC/DHDAB bilayer system, the vesicles with $X_{\text{DHDAB}} \geq 0.1$ exhibited positive zeta potentials of ~50 mV and smaller particle size with narrower size distribution than those of pure DSPC vesicles. Furthermore, fluorescence polarization measurements indicated that incorporation of DHDAB into DSPC bilayers with X_{DHDAB} from 0.1 to 0.5 increased the membrane rigidity. Besides, adding DHDAB into DSPC vesicles can improve the stability of pure DSPC vesicles and the most stable vesicle appeared at $X_{\text{DHDAB}} = 0.5$ because of the optimization between intervesicle and intravesicle interactions. Findings from monolayers like the condensing effect and the enhanced molecular interactions and packing may help explain that the stability of mixed DSPC/DHDAB vesicles is better than that of vesicles of pure components without considering electrostatic repulsion of intervesicles. The results suggest that the most stable vesicle with $X_{\text{DHDAB}} = 0.5$ has potential to be used in drug delivery and/or gene transfection.

AUTHOR INFORMATION

Corresponding Author

*E-mail: chouth@yuntech.edu.tw; Tel: (+) 886-5-5342601 ext 4625; Fax: (+) 886-5-5312071.

Notes

The authors declare no competing financial interest.

ACKNOWLEDGMENTS

This study was supported by the National Science Council of Taiwan through Grants NSC96-2221-E041-019-MY2 and NSC 98-2622-E-041-011-CC3.

REFERENCES

- (1) Carmona-Ribeiro, A. M. *Curr. Med. Chem.* **2003**, *10*, 2425–2446.
- (2) Ruozzi, B.; Forni, F.; Battini, R.; Vandelli, M. A. *J. Drug Target.* **2003**, *11*, 407–414.
- (3) Montier, T.; Benvegnù, T.; Jaffrès, P. A.; Yaouanc, J. J.; Lehn, P. *Curr. Gene Ther.* **2008**, *8*, 296–312.
- (4) Morille, M.; Passirani, C.; Vonarbourg, A.; Clavreul, A.; Benoit, J.-P. *Biomaterials* **2008**, *29*, 3477–3496.
- (5) Barteau, B.; Chèvre, R.; Letrou-Bonneval, E.; Labas, R.; Lambert, O.; Pitard, B. *Curr. Gene Ther.* **2008**, *8*, 313–323.
- (6) Llères, D.; Weibel, J. M.; Heissler, D.; Zuber, G.; Duportail, G.; Mély, Y. *J. Gene Med.* **2004**, *6*, 415–428.
- (7) Lv, H.; Zhang, S.; Wang, B.; Cui, S.; Yan, J. *J. Controlled Release* **2006**, *114*, 100–109.
- (8) Liang, C.-H.; Chou, T.-H. *Chem. Phys. Lipids* **2009**, *158*, 81–90.
- (9) Sakurai, F.; Inoue, R.; Nishino, Y.; Okuda, A.; Matsumoto, O.; Taga, T.; Yamashita, F.; Takakura, Y.; Hashida, M. *J. Controlled Release* **2000**, *66*, 255–269.
- (10) Ramezani, M.; Khoshhamdam, M.; Dehshahri, A.; Malaekeh-Nikouei, B. *Colloids Surf., B* **2009**, *72*, 1–5.
- (11) Dass, C. R.; Walker, T. L.; Burton, M. A. *Drug Delivery* **2002**, *9*, 11–18.
- (12) Pacheco, L. F.; Carmona-Ribeiro, A. M. *J. Colloid Interface Sci.* **2003**, *258*, 146–154.
- (13) Jones, M. N. *Methods Enzymol.* **2005**, *391*, 211–228.
- (14) Manosroi, A.; Thathang, K.; Manosroi, J.; Werner, R. G.; Schubert, R.; Peschka-Süss, R. *J. Liposome Res.* **2009**, *19*, 131–140.
- (15) Sobral, C. N.; Soto, M. A.; Carmona-Ribeiro, A. M. *Chem. Phys. Lipids* **2008**, *152*, 38–45.
- (16) Linseisen, F. M.; Bayerl, S.; Bayerl, T. M. *Chem. Phys. Lipids* **1996**, *83*, 9–23.
- (17) Montalvo, G.; Valiente, M.; Khan, A. *Langmuir* **2007**, *23*, 10518–10524.
- (18) Tucker, I.; Penfold, J.; Thomas, R. K.; Grillo, I.; Barker, J. G.; Mildner, D. F. R. *Langmuir* **2008**, *24*, 6509–6520.
- (19) Almeida, P. F. F. *Biochim. Biophys. Acta* **2009**, *1788*, 72–85.
- (20) Ho, E. A.; Ramsay, E.; Ginj, M.; Anantha, M.; Bregman, I.; Sy, J.; Woo, J.; Osooly-Talesh, M.; Yapp, D. T.; Bally, M. B. *J. Pharm. Sci.* **2010**, *99*, 2839–2853.
- (21) Herrington, T. P.; Altin, J. G. *Int. J. Pharm.* **2011**, *411*, 206–214.
- (22) Pedroso de Lima, M. C.; Neves, S.; Filipe, A.; Düzgüneş, N.; Simões, S. *Curr. Med. Chem.* **2003**, *10*, 1221–1231.
- (23) Leblanc, R. M. *Curr. Opin. Chem. Biol.* **2006**, *10*, 529–536.
- (24) Gonçalves da Silva, A. M.; Romão, R. I. *Chem. Phys. Lipids* **2005**, *137*, 62–76.
- (25) Bordi, F.; Cametti, C.; Di Venanzio, C.; Sennato, S.; Zuzzi, S. *Colloids Surf., B* **2008**, *61*, 304–310.
- (26) Chou, T.-H.; Lin, Y.-S.; Li, W.-T.; Chang, C.-H. *J. Colloid Interface Sci.* **2008**, *321*, 384–392.
- (27) Campbell, R. B.; Balasubramanian, S. V.; Straubinger, R. M. *Biochim. Biophys. Acta* **2001**, *1512*, 27–39.
- (28) Chou, T.-H.; Chu, I.-M.; Chang, C.-H. *Colloids Surf., B* **2002**, *25*, 147–155.
- (29) Li, W.-T.; Yang, Y.-M.; Chang, C.-H. *Colloids Surf., B* **2008**, *66*, 187–194.
- (30) Tamai, N.; Uemura, M.; Takeichi, T.; Goto, M.; Matsuki, H.; Kaneshina, S. *Biophys. Chem.* **2008**, *135*, 95–101.
- (31) Feitosa, E.; Jansson, J.; Lindman, B. *Chem. Phys. Lipids* **2006**, *142*, 128–132.
- (32) Gaines Jr., G. L. *Insoluble Monolayers at Liquid–Gas Interfaces*; Wiley-Interscience: New York, 1966; Chapter 6.
- (33) Holopainen, J. M.; Brockman, H. L.; Brown, R. E.; Kinnunen, P. K. J. *Biophys. J.* **2001**, *80*, 765–775.
- (34) Oliveira, O. N.; Bonardi, C. *Langmuir* **1997**, *13*, 5920–5924.
- (35) Birdi, K. S. *Lipid and Biopolymer Monolayers at Liquid Interfaces*; Plenum Press: New York, 1989; Chapter 4.
- (36) Chou, T.-H.; Chang, C.-H. *Langmuir* **2000**, *16*, 3385–3390.
- (37) Gurtovenko, A. A.; Patra, M.; Karttunen, M.; Vattulainen, I. *Biophys. J.* **2004**, *86*, 3461–3472.
- (38) Zhao, W.; Gurtovenko, A. A.; Vattulainen, I.; Karttunen, M. *J. Phys. Chem. B* **2011**, *116*, 269–276.
- (39) Säily, V. M. J.; Alakoskela, J.-M.; Ryhänen, S. J.; Karttunen, M.; Kinnunen, P. K. J. *Langmuir* **2003**, *19*, 8956–8963.
- (40) Goloub, T. P.; Pugh, R. J.; Zhmud, B. V. *J. Colloid Interface Sci.* **2000**, *229*, 72–81.
- (41) Razavizadeh, B. M.; Mousavi-Khoshdel, M.; Gharibi, H.; Behjatmanesh-Ardakani, R.; Javadian, S.; Sohrabi, B. *J. Colloid Interface Sci.* **2004**, *276*, 197–207.
- (42) Flores, A.; Ize, P.; Ramos, S.; Castillo, R. *J. Chem. Phys.* **2003**, *119*, 5644–5653.
- (43) Karttunen, M.; Haataja, M. P.; Säily, M.; Vattulainen, I.; Holopainen, J. M. *Langmuir* **2009**, *25*, 4595–4600.
- (44) Cárdenas, M.; Nylander, T.; Jönsson, B.; Lindman, B. *J. Colloid Interface Sci.* **2005**, *286*, 166–175.
- (45) Dabkowska, A. P.; Barlow, D. J.; Hughes, A. V.; Campbell, R. A.; Quinn, P. J.; Lawrence, M. J. *J. R. Soc. Interface* **2011**, DOI: 10.1098/rsif.2011.0356.
- (46) Keller, D. J.; McConnell, H. M.; Moy, V. T. *J. Phys. Chem.* **1986**, *90*, 2311–2315.
- (47) Keller, D. J.; Korb, J. P.; McConnell, H. M. *J. Phys. Chem.* **1987**, *91*, 6417–6422.
- (48) Flores, A.; Corvera-Poiré, E.; Garza, C.; Castillo, R. *J. Phys. Chem. B* **2006**, *110*, 4824–4835.
- (49) Yokoyama, S.; Inagaki, A.; Imura, T.; Ohkubo, T.; Tsubaki, N.; Sakai, H.; Abe, M. *Colloids Surf., B* **2005**, *44*, 204–210.
- (50) Lentz, B. R. *Chem. Phys. Lipids* **1989**, *50*, 171–190.
- (51) Lentz, B. R. *Chem. Phys. Lipids* **1993**, *64*, 99–116.